Chemical Geology 646 (2024) 121896

Contents lists available at ScienceDirect

Chemical Geology

journal homepage: www.elsevier.com/locate/chemgeo

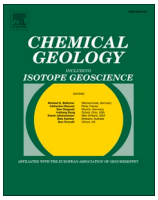

Refining the carbonate-associated iodine redox proxy with leaching experiments

Kun Zhang *, Gary Tarbuck, Graham A. Shields

Department of Earth Sciences, University College London, WC1E 6BT, UK

ARTICLE INFO

Editor: Don Porcelli

Keywords:
Iodine
Redox
Carbonate
Leaching
Oxygenation

ABSTRACT

Iodate ions can substitute for carbonate in crystal lattices, which is why carbonate-associated iodine (CAI) is increasingly being used to track redox-sensitive iodine species, and by extrapolation, the redox conditions of ancient oceans. Extracting iodine from carbonate rocks is challenging, however, because iodine is susceptible to volatilization in acidic solutions. A broadly similar leaching scheme with different leaching times has been applied to all kinds of ancient carbonate rocks. However, the effects of non-carbonate phases and iodine stability during leaching remain under-constrained, which limits its use for paleoredox reconstruction. For this study, we assessed these issues by conducting a series of leaching experiments on carbonate standards and ancient carbonate rocks of varying purity. We first developed an alternative stabilizer for iodine, i.e., 3% EDTA (ethylenediaminetetraacetic acid) in 3% NH_4OH (ammonium hydroxide). This easily accessible new stabilizer effectively prevents the precipitation of metal ions from the alkaline solution, thus easing the preparation process and reducing the iodine signal drift during the CAI analysis. We also propose two interlaboratory limestone standards for iodine analysis with long-term (one year) I/Ca values of 0.43 ± 0.03 μmol/mol for limestone CRM-393 and 0.99 ± 0.06 μmol/mol for argillaceous limestone SRM-1c. Here we demonstrate that excessive leaching times (>60 min) can lead to the loss of nearly half of the iodine released under typical leaching conditions. Bulk carbonate digestion is shown to potentially underestimate primary CAI concentrations due to the presence of diagenetic carbonates. Moreover, we identified phosphates and organic matter as potential contaminants, the inadvertent leaching of which could lead to overestimated concentrations. Although the potential significance of such contamination warrants further study, our results show that contamination, if present, can be minimised by oxidative cleaning with 12% NaClO followed by dissolution in 0.3 M acetic acid. The possibility that measured CAI concentrations can be both under- and over-estimated may lead to reassessment of oxygenation events identified from the iodine concentrations of impure carbonate rocks.

1. Introduction

Because atmospheric-oceanic redox conditions are intimately linked to biotic evolution and the global carbon cycle, geochemical paleoredox proxies have received considerable attention (e.g., Lyons et al., 2014; Lenton et al., 2014; Alcott et al., 2019). Several carbonate rock-based geochemical proxies have been developed and used to infer redox states of the water column or the sediment-water interface in deep time, including U isotopes ($\delta^{238}U$), S isotopes ($\delta^{34}S$), Ce anomaly, and iodine content (Webb and Kamber, 2000; Hurtgen et al., 2002; Lu et al., 2010; Wotte et al., 2012; Andersen et al., 2014; Hardisty et al., 2014; Lau et al., 2016; Tostevin et al., 2016; Zhang et al., 2020; Zhang and Shields, 2022). Of these proxies, $\delta^{34}S$ is indirectly linked to Earth's surface redox state by tracking the pyrite burial fraction, while $\delta^{238}U$ provides direct insight into global marine redox states (e.g., Lau et al., 2016; He et al., 2019; Fakhraee et al., 2019; Zhang et al., 2020). The Ce anomaly and carbonate-associated iodine (CAI, hereafter) are the only two widely applied proxies in carbonate rocks that relate to local to regional shallow marine redox conditions. The iron speciation, a commonly used local redox proxy in shales, can also be applied to carbonate rocks, but only if total iron content is high (>0.5 wt%), and is less sensitive to more oxidising conditions (e.g., Poulton and Canfield, 2005; Clarkson et al., 2014; Tostevin et al., 2016). The application of the Ce anomaly as a paleoredox proxy is built upon the redox sensitivity of the Ce(III) / Ce(IV) transition and their contrasting solubilities (De Baar et al., 1985; German and Elderfield, 1990; Sholkovitz et al., 1994). Yet,

* Corresponding author.
E-mail address: kun.zhang.19@ucl.ac.uk (K. Zhang).

https://doi.org/10.1016/j.chemgeo.2023.121896
Received 30 September 2023; Received in revised form 8 December 2023; Accepted 15 December 2023
Available online 17 December 2023

interpretation of Ce anomalies is not always straightforward. The magnitude of the Ce anomaly may vary with oxygen availability, water depth and pH, as well as local particulate flux, and may be overprinted during diagenesis (Kamber et al., 2014; Bellefroid et al., 2018; Tostevin, 2021; Cao et al., 2022; Zhang and Shields, 2023). Moreover, extracting rare earth elements (REE; and Ce anomalies) from carbonate rocks is challenging because non-carbonate phases such as silicates, phosphates, Fe/Mn oxides and organic matter are enriched in REE and can easily contaminate carbonate REE signals. Although sequential leaching enables the least contaminated carbonate phase to be targeted, it is usually not applicable to impure carbonate rocks (Zhang et al., 2015; Tostevin et al., 2016; Cao et al., 2020; Zhang and Shields, 2023). Therefore, a complementary proxy is required to better constrain local-regional redox conditions in deep time.

Carbonate-associated iodine (expressed as I/Ca or I/(Ca + Mg)), a promising redox proxy, is developed based on the redox sensitivity of iodine speciation in modern oceans. Dissolved inorganic iodine mainly comprises two thermodynamic stable species in seawater: oxidised iodate (IO_3^-) and reduced iodide (I^-). Although iodine has a relatively conservative total inorganic concentration of 450–500 nM and hence a relatively long residence time of ~300 kyr in the modern ocean, the concentrations of different iodine species largely depend on the seawater redox potential (Wong and Brewer, 1977; Broecker and Peng, 1982; Rue et al., 1997; Cutter et al., 2018). The reduction of iodate to iodide through assimilatory and dissimilatory processes is considered to be more rapid than the reverse oxidation (Chance et al., 2014; Hardisty et al., 2021). Iodate is thus prevalent in oxic seawater and significantly diminished in more reducing seawater (e.g., oxygen minimum zones). However, regional water mass mixing can still lead to elevated iodate concentrations (>350 nM) in seawater with dissolved oxygen concentrations lower than 1 μM (Hardisty et al., 2021), indicating that local iodate concentrations may also be a function of ocean circulation.

Laboratory precipitation experiments and X-ray absorption data demonstrate that only IO_3^- is incorporated into calcite and dolomite lattices by substituting for the CO_3^{2-} ion (Lu et al., 2010; Podder et al., 2017; Kerisit et al., 2018; Hashim et al., 2022). Consequently, CAI concentrations can potentially track iodate concentrations and hence, redox conditions of ambient fluids from which carbonate minerals precipitated. Since seawater iodate concentration variation is dictated by oxygen availability, primary production and ocean circulation (Lu et al., 2010; Lu et al., 2016; Hardisty et al., 2021), CAI is mostly regarded as a local-regional redox proxy. Additionally, because the oxidation potential of the IO_3^-/I^- couple is relatively high, and similar to the Mn or Ce redox couples, the proxy is expected to respond to hypoxia or suboxia (the threshold of hypoxia may vary with marine organism species and here hypoxia refers to $O_2 < 70–100$ μM, and suboxic refers to $O_2 < 5–10$ μM; Rue et al., 1997; Lu et al., 2010; Lu et al., 2020a). Given its great potential to reconstruct oceanic redox changes, the iodine proxy has been applied to ancient carbonate rocks from the Archean to the Phanerozoic (e.g., Lu et al., 2010; Loope et al., 2013; Hardisty et al., 2014; Lu et al., 2018; Shang et al., 2019; Wörndle et al., 2019; He et al., 2022).

Attempts have also been made to link CAI concentrations directly to dissolved oxygen levels. For example, it has been proposed that a foraminiferal I/Ca <2.5–3.0 μmol/mol may indicate dissolved O_2 concentration < 20–70 μM (Lu et al., 2016; Lu et al., 2022). However, it has been observed that low planktic foraminiferal I/Ca values (<2.5 μmol/mol) co-occur with locally high dissolved O_2, possibly as a result of the slow kinetics of iodide oxidation (Lu et al., 2020a). High water column IO_3^- concentration alongside locally negligible dissolved O_2 due to water mass mixing has also been reported (Hardisty et al., 2021). Furthermore, although both calcite and dolomite can accommodate iodate in their respective crystal lattices, the partition coefficient of iodate is smaller for dolomite (Hashim et al., 2022). Differences in iodine concentrations of limestones and dolostones could therefore be caused by differences in primary mineralogy, together with fluid- versus sediment-buffered conditions during diagenetic recrystallization, instead of fluid iodate concentrations alone. Diagenetic alteration also tends to decrease CAI concentrations (Loope et al., 2013; Hardisty et al., 2017). Although secondary carbonates precipitated from highly oxidising fluids may theoretically have even higher iodine concentrations than primary carbonates, such a case has not been reported in geological samples. Together, these considerations hinder any direct application of CAI as a quantitative proxy for local dissolved oxygen levels (Lu et al., 2020a).

Despite such caveats, robust increases in CAI concentrations from a low baseline are widely thought to reflect greater iodate (and oxygen) availability in seawater. However, an apparent rise in iodine concentrations could also be the result of inadvertent leaching of non-carbonate phases, leading potentially to misinterpretation. Therefore, it is critical to refine the leaching method to better apply the qualitative CAI redox proxy. Published CAI studies have employed a broadly similar leaching strategy since the proxy was first developed by Lu et al. (2010). In general, a small amount of carbonate sample powder is cleaned with ultrapure water, completely dissolved by dilute nitric acid (mostly 3% HNO_3), followed by iodine stabilization using an alkaline stabilizer. However, because carbonate-associated iodine is a concentration-based proxy, great care should be taken during carbonate sample leaching for several reasons. First, iodine is susceptible to volatilization in acidic conditions due to the formation of volatile HOI and/or I_2 resulting from the reactions of iodine species with H^+ (e.g., Schmitz, 2000). While 3% HNO_3 has been typically used for carbonate dissolution, published leaching times vary from 10 min to as long as overnight (e.g., Hardisty et al., 2017). As iodine loss during leaching is yet to be explicitly explored, it remains to be shown that results using different methods are comparable. Second, dilute nitric acid leaching has the potential to attack non-carbonate phases (Cao et al., 2020). Although nitric acid leaching has been applied as standard to both pure and impure organic-rich carbonate rocks (e.g., Wei et al., 2019; Huang et al., 2022; He et al., 2022), it has also been demonstrated that organic matter oxidation can lead to elevated foraminiferal I/Ca values (Glock et al., 2019; Winkelbauer et al., 2021). Unlike for foraminifera, the influence of non-carbonate phases on measured CAI in ancient carbonate rocks has not been investigated systematically. Moreover, the commonly used alkaline stabilizers are either extremely toxic and not easily accessible or may trigger precipitation of metal ions, such as calcium and magnesium, thus leading to the need for meticulous preparation protocols and possible instrument drift during analysis. It is desirable therefore to scrutinise the robustness of the CAI leaching method, and if possible establish a standardised leaching procedure for CAI studies.

For this study, we first developed an easily accessible stabilizer suitable for large batch analysis of carbonate rocks with low iodine contents by increasing the matrix concentration (e.g., ~100 ppm Ca), further expanding the application of the proxy. We then performed a series of leaching experiments to assess the effects of leaching time, non-carbonate phases, acid strength, and sequential leaching on measured CAI. Based on our experiments, we propose a leaching protocol for iodine analysis in ancient carbonate rocks, thus refining the utility of carbonate-associated iodine as a paleoredox proxy. Finally, we recommend two limestone reference materials as interlaboratory standards for iodine analysis.

2. Materials and methods

2.1. Samples and reagents

Carbonate rocks of varying purity were collected from the Mesoproterozoic Tieling and Gaoyuzhuang formations on the North China Craton. Carbonate rocks from these units have been previously reported to contain relatively high iodine concentrations against a low background value (Hardisty et al., 2017; Shang et al., 2019). Sample powder was produced using a microdrill or an agate TEMA mill, avoiding

weathered surfaces and veins. Samples from the Gaoyuzhuang Formation were collected from its member III at Gan'gou section, and consist of organic-rich, variably dolomitised, impure carbonates with a mean carbonate content of 58% and a mean total organic carbon (TOC) of 1.22%. Samples from the Tieling Formation at Jixian section comprise relatively pure limestones and dolostones with a mean carbonate content of 88%. In addition, certified reference materials including JCp-1 (coral, *Porites* sp.; from GSJ), BAM RS-3 (calcite; from BAM), CRM-393 (limestone; from BAS), SRM-88a (dolomitic limestone; from NIST), SRM-1c (argillaceous limestone; from NIST), SGR-1 (green river shale; from USGS) and phosphorite SRM-120b (Florida phosphate rock; from NIST) were used in different sets of leaching experiments as described in the following.

Ethylenediaminetetraacetic acid (EDTA; purified grade, ≥98.5%) and potassium iodate powder (99.995% trace metals basis) were purchased from Sigma-Aldrich. Hydrogen peroxide (60%) was bought from Fisher Scientific. Sodium hypochlorite (14%) was supplied by VWR. Nitric acid was distilled using Savillex DST-1000 Teflon stills before being diluted with deionized water (18.2 MΩ·cm). Acetic acid was diluted from ROMIL-UpA glacial acetic acid (>99%), while ammonia solution was diluted from VWR AnalaR ammonia solution (28%) or ROMIL-UpA ammonia solution (20–22%).

2.2. Leaching experiments

Leaching experiments were divided into several groups of comparative trials for different purposes (Table 1). To optimise the stabilizer for relatively high matrix concentrations (e.g., 100 ppm Ca) prepared for relatively low instrument sensitivity and low-iodine analysis, the first group applied the same leaching method to certified standards, including coral JCp-1, calcite BAM RS-3, limestone CRM-393, dolomitic limestone SRM-88a and argillaceous limestone SRM-1c. Approximately 5 mg of sample powder was weighed into acid-cleaned polypropylene tubes and leached with 1 ml 3% HNO_3. The leaching was kept within 10 min for coral JCp-1 and 20 min for other standards to minimise any potential iodine volatilization (also see the following setup). The samples were then centrifuged, and aliquots of supernatants diluted in the stabilizer immediately for elemental analysis. In total, we conducted four independent batches of leaching experiments to evaluate different stabilizers, including 3% (w/v) NH_4OH, 0.5% (w/v) EDTA in 3% (w/v) NH_4OH, 1% (w/v) EDTA in 3% (w/v) NH_4OH, and 3% (w/v) EDTA in 3% (w/v) NH_4OH. For each certified standard, iodine was measured at least six times during each batch analysis to monitor the precision and long-term drift. For comparison, we also conducted an independent test by monitoring the drift monitor (with known iodine concentration) after measuring every seven unknown samples, which were all diluted in 0.5% (w/v) EDTA in NaOH solution. Once the stabilizer was optimised, all the following leaching experiments used the same stabilizer for iodine analysis.

To assess the potential influence of leaching time on measured iodine concentrations, the second group comprised six relatively pure limestones and dolostones from the ca. 1.44 Ga Tieling Formation. ~5 mg of sample powder was first rinsed with 1 ml deionized (DI) water under ultrasonication for 10 min. The supernatants were discarded following centrifugation (4000 rpm, 3 min) and residues leached with 1 ml 3% HNO_3 in an ultrasonic bath. For five independent batches, the leaching time was set at 10, 15, 30, 60 and 120 min. Samples were then centrifuged and aliquots of supernatants diluted in the stabilizer immediately for elemental analysis.

For the third group, we conducted oxidative cleaning before leaching in order to evaluate the effect of organic matter on measured iodine contents. Six impure dolomitised carbonate rocks (mean TOC 1.22%) from the ca. 1.56 Ga Gaoyuzhuang Formation were selected and the pure limestone CRM-393 was also used for comparison. For each sample, approximately 20 mg of sample powder was weighed. In five independent batches, samples were cleaned respectively with 2 ml DI water once, 12% (w/v) NaClO once and twice, 1% H_2O_2 (w/v) in 0.1 M NaOH (buffered H_2O_2) once and twice under ultrasonication for 10 min. The H_2O_2 is buffered with alkali in order to reduce carbonate dissolution before leaching (Barker et al., 2003), and we note that the buffered 1% H_2O_2 solution was not heated as is commonly done (Lu et al., 2016). The bleached samples were further rinsed with DI water three times with the help of a vortex mixer to remove reagents. After cleaning, all residues were leached with 2 ml 3% HNO_3 in an ultrasonic bath for 15 min, followed by centrifugation. Aliquots of supernatants were diluted in the stabilizer immediately for elemental analysis.

The fourth group was designed to assess the effect of phosphates and silicate minerals on extracted iodine contents. It includes two sets of samples, with one set comprising six impure dolomitised carbonate rocks from the Gaoyuzhuang Formation and three pure dolostones (carbonate contents >90%) from the Tieling Formation. The other set includes coral JCp-1, limestone CRM-393, argillaceous limestone SRM-1c, and their mixtures with one of the certified standards shale SGR-1 and phosphorite SRM-120b, respectively. The mixing ratios ranged from 20% to 35%. Approximately 4–8 mg of sample powder was weighed. For impure and pure dolostones, samples were cleaned with 1 ml DI water in the ultrasonic bath for 10 min, then leached with 1 ml 3% HNO_3 or 0.3 M acetic acid in two independent batches for 15 min under ultrasonication. For certified standards and artificially made impure carbonate rocks, samples were leached directly with 1 ml 3% HNO_3 or 0.3 M acetic acid in two independent batches for 10 min in the ultrasonic bath. Leachates were centrifuged and diluted in the stabilizer immediately for elemental analysis.

Finally, nine carbonate rocks were selected for sequential leaching, including pure limestones and pure and impure dolostones from the Gaoyuzhuang and Tieling formations. ~40 mg of sample powder was cleaned with 2 ml DI water in the ultrasonic bath for 10 min. Samples were then leached for 15 min with a certain amount of 3% HNO_3

Table 1
Brief summary of samples, procedures, acids and stabilizers used throughout this study.

Group	Samples	Cleaning	Leaching time	Leaching acid	Stabilizer
1	JCp-1, BAM RS-3, CRM-393, SRM-88a, SRM-1c	–	Within 20 min	3% HNO_3	3% NH_4OH, 0.5% EDTA in 3% NH_4OH, 1% EDTA in 3% NH_4OH, 3% EDTA in 3% NH_4OH
2	Tieling	DI water	10, 15, 30, 60, 120 min	3% HNO_3	3% EDTA in 3% NH_4OH
3	Gaoyuzhuang, CRM-393	DI water, 12% NaClO, buffered H_2O_2 (unheated)	15 min	3% HNO_3	3% EDTA in 3% NH_4OH
4	JCp-1, CRM-393, SRM-1c, and their mixtures with SGR-1 and SRM-120b	–	10 min	3% HNO_3, 0.3 M acetic acid	3% EDTA in 3% NH_4OH
	Tieling, Gaoyuzhuang	DI water	15 min	3% HNO_3, 0.3 M acetic acid	3% EDTA in 3% NH_4OH
5	Tieling, Gaoyuzhuang	DI water	15 min	Sequential leaching with 3% HNO_3	3% EDTA in 3% NH_4OH

sequentially in an ultrasonic bath. Aliquots of supernatants were then diluted in the stabilizer immediately for elemental analysis, while the residues after each leaching step were rinsed with DI water three times.

2.3. Elemental analysis

Stabilized supernatants were diluted in the stabilizer for Ca and Mg analyses using a Varian 720 inductively coupled plasma optical emission spectrometer (ICP-OES) at University College London. Shale SGR-1 and dolomitic limestone SRM-88a that were subjected to bulk digestion as in-house solution standards were analysed routinely to monitor the accuracy. The precisions and accuracies for Ca and Mg were typically better than 5% and blanks were negligible. Based on measured Ca concentrations, stabilized supernatants were further diluted in the stabilizer to contain ~100 ppm Ca. This Ca matrix concentration is higher than that normally used in CAI studies (i.e., 50 ppm Ca) because our samples have relatively low iodine concentrations, and the I-127 sensitivity in our instrument is not exceptionally high. Solutions were then analysed for iodine with an Agilent 7900 inductively coupled plasma mass spectrometer (ICP-MS) at University College London. 2 ppb indium was spiked beforehand as an internal standard to monitor the instrumental drift and matrix effects. The potential memory effect caused by iodine vaporisation was eliminated by aspirating the 7 M ammonia solution after the uptake of sample solutions. Calibration standards were made freshly from potassium iodate powder, dissolved in the stabilizer with 100 ppm Ca matched to samples. A drift monitor (0.1 ppb iodine calibration standard solution) and coral JCp-1 were analysed repeatedly during each batch analysis to check the instrumental drift. The sensitivity of I-127 was typically 60–70 kcps (thousand counts per second) for the 1 ppb standard. The detection limit of I/Ca is ~0.1 μmol/mol. The instrument precision for iodine was typically better than 3%. Analysis of coral JCp-1 duplicates yielded I/Ca values of 4.13 ± 0.21 μmol/mol (1SD, n = 12), comparable to published literature values (Lu et al., 2020b). The iodine concentrations of stabilizers and procedure blanks were all below the detection limit, ruling out any measurable effect of iodine addition from ambient air due to I_2 hydrolysis in a very alkaline solution (Cook et al., 2022).

3. Results and discussion

3.1. Optimisation of stabilizer

Due to iodine volatilization in acidic solutions, an alkaline solution is usually added to stabilize iodine immediately after sample leaching. Commonly used stabilizers include tertiary amine (Lu et al., 2010; Hardisty et al., 2017; Lu et al., 2018; Pohl et al., 2021) and tetramethylammonium hydroxide (TMAH; Takaku et al., 1995; Glock et al., 2014; Winkelbauer et al., 2021; Cook et al., 2022). Although these stabilizers are known to be effective, they are toxic and not easily accessible. Ammonium hydroxide (NH_4OH) has also been used as a stabilizer (e.g., Winkelbauer et al., 2021; He et al., 2022). However, the mixture of an alkaline solute with abundant Ca^{2+} and/or Mg^{2+} derived from carbonate leaching may trigger metal precipitation. This requires iodine analysis to be performed therefore often immediately after the leaching process. Salt precipitation could also potentially cause severe and irregular instrumental drifts that are difficult to correct during ICP-MS analysis (Agatemor and Beauchemin, 2011).

In this study, we assessed the effectiveness of a mixture of EDTA with NH_4OH as a stabilizer. EDTA is a readily accessible, mildly acidic and low-toxicity tertiary amine. As a strong chelating reagent, EDTA can form stable complexes with metals like Ca^{2+} and Mg^{2+} (e.g., Byegård et al., 1999) and thus could potentially preclude their precipitation in the alkaline solution and mitigate the drift during analysis. NH_4OH facilitates EDTA dissolution, which is otherwise insoluble in water, and produces an alkaline solution to stabilize iodine. In some cases, sodium hydroxide (NaOH) is also utilized to stabilize iodine (see review in Flores et al., 2020). We thus also prepared a 0.1 ppb iodine standard solution stabilized with 0.5% EDTA in NaOH to test its effectiveness for iodine measurement (see Section 2.2). The measured iodine intensity decreased significantly during the ICP-MS analysis (Fig. S1). Given the concomitantly decreased intensity of non-volatile indium (Fig. S1), the continuous signal drift is most likely induced by matrix effects caused by the abundant Na^+ in the solution (~1600 ppm). Therefore, our results echo the well-known phenomenon of signal depression under high Na^+ concentration, possibly due to salt deposition on cones (Cheatham et al., 1993; Agatemor and Beauchemin, 2011). As a result, we consider that NaOH is not an ideal stabilizer for iodine analysis.

Iodine concentrations of coral JCp-1 obtained using NH_4OH and mixtures with EDTA as stabilizers show I/Ca of 3.92 ± 0.10 μmol/mol (1SD, n = 4), which is calculated based on only the first measurement in each batch analysis due to the presumably lowest instrumental drift. The values are consistent with literature values obtained using other stabilizers (e.g., Chai and Muramatsu, 2007; Glock et al., 2014; Lu et al., 2020b), suggesting that our stabilizers are capable of stabilizing iodine. Calcite BAM RS-3 and dolomitic limestone SRM-88a show iodine concentrations below the detection limit, while limestone CRM-393 and argillaceous limestone SRM-1c have I/Ca values of 0.42 ± 0.05 μmol/mol and 0.96 ± 0.09 μmol/mol, respectively. The detectable iodine in the two limestone standards is promising as their concentrations are close to those of Precambrian carbonate rocks, making them particularly useful for assessing the data accuracy (also see Section 3.6). Fig. 1 shows the variation of measured iodine concentrations of the drift monitor and standards in different stabilizers during each batch analysis. Although we do not observe the significant drift that was evident using 0.5% EDTA with NaOH, measured iodine concentrations show systematic variation in different stabilizers. First, there is still a tendency for measured iodine concentrations to decrease over time, indicating the presence of continuous signal depression, due possibly to salt deposition (Fig. 1). Second, the effect of instrumental drift (expressed as the relative standard deviation of repeated analyses in each batch; RSD) varies with the iodine concentrations of samples, which is typically larger for the drift monitor and limestone CRM-393 (Table 2). This implies that rock samples with low iodine concentrations (e.g., Precambrian carbonate rocks) are particularly prone to instrumental drifts, thus resulting in relatively high data uncertainty. Third, the drift also varies with the concentration of EDTA. The most obvious drift is observed in 3% NH_4OH without EDTA, whereby the iodine concentration of the drift monitor decreases from 0.31 to 0.23 μmol/mol with an RSD of 11.6% (Fig. 1 and Table 2). With increasing EDTA concentrations, the instrumental drifts for the drift monitor and certified standards decrease systematically, confirming that EDTA efficiently reduced salt deposition even in alkaline solutions (Table 2).

It has been shown that the iodine signal can be enhanced by adding isopropanol and methanol to the matrix (Ariga et al., 2019; He et al., 2022). Carbon-induced signal enhancement is often attributed to the presence of carbon species that increases the analyte ionization efficiency through charge transfer or increase atomization efficiency through analyte oxide reduction by CO formation (Agatemor and Beauchemin, 2011; Ariga et al., 2019). The source of carbon is not crucial to signal enhancement (Grindlay et al., 2013), and hence, it is expected that EDTA may also be able to increase signal intensity. However, we did not observe significant intensity variation for the drift monitor, although the intensity gradually increased from 57 to 74 kcps for the 1 ppb standard solution with increasing EDTA concentrations (Fig. 2). Nonetheless, the background intensity was not influenced by EDTA concentrations and the detection limit remained unaffected (~0.1 μmol/mol). Taken together, considering the low toxicity, good reproducibility, and signal stability over long-time measurement, we suggest that 3% EDTA in 3% NH_4OH is a suitable alternative stabilizer for the large batch analysis of carbonate rocks with low iodine contents. This reagent has been used for all the following leaching experiments.

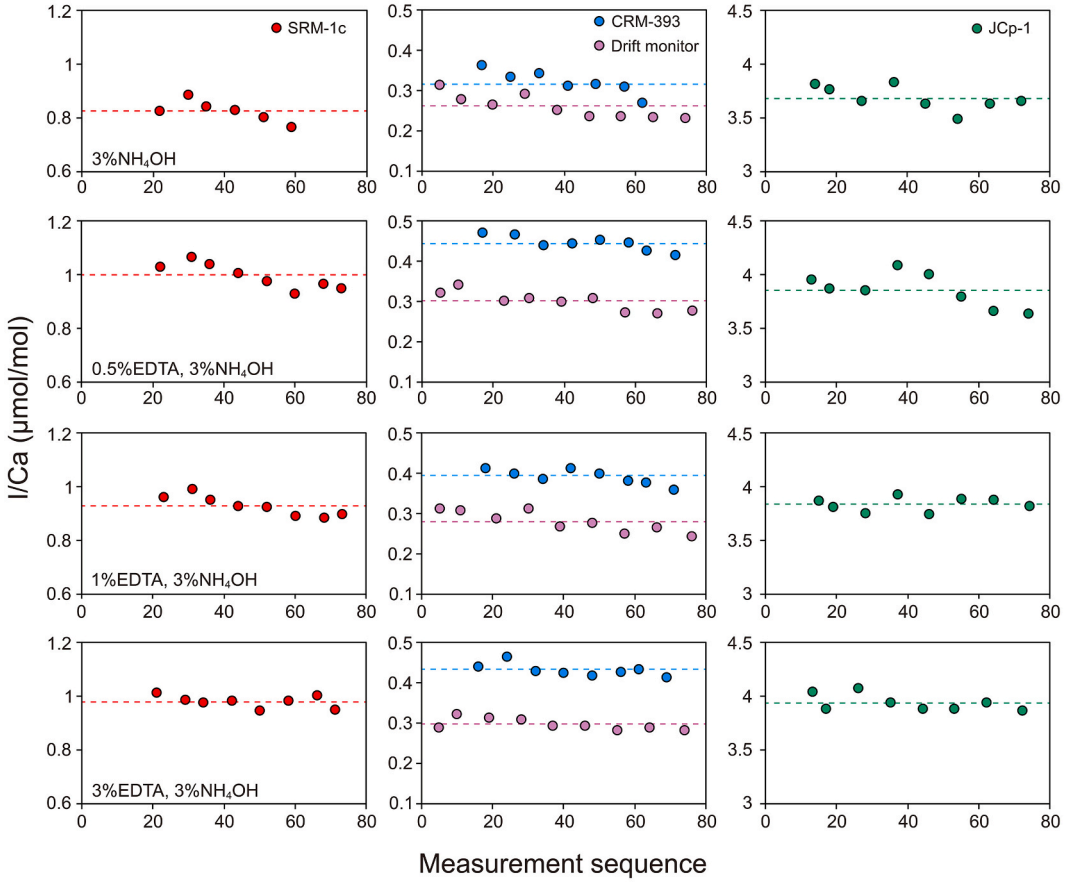

Fig. 1. Repeated iodine measurement results for the argillaceous limestone SRM-1c (red), drift monitor (purple), limestone CRM-393 (blue), and coral JCp-1 (green) in each batch analysis. Each row represents the results from the same batch, while different rows indicate different batches with different stabilizers, shown in the left columns, used in both samples and calibration standards for iodine analysis. Iodine concentrations are shown as I/Ca based on measured Ca in corresponding leachates on ICP-OES. The Ca concentration of the drift monitor is 100 ppm. Dashed lines indicate the mean values of repeated measurements. (For interpretation of the references to colour in this figure legend, the reader is referred to the web version of this article.)

Table 2
Mean I/Ca ratios (μmol/mol) of the drift monitor and carbonate standards in each batch analysis. The values in brackets indicate standard deviations (1SD) and numbers of measurements, respectively.

Stabilizer	Drift monitor		CRM 393		SRM-1c		JCp-1	
	Mean I/Ca	RSD	Mean I/Ca	RSD	Mean I/Ca	RSD	Mean I/Ca	RSD
3% NH_4OH	0.26 (0.03, n = 9)	11.6%	0.32 (0.03, n = 7)	9.2%	0.83 (0.04, n = 6)	4.8%	3.69 (0.11, n = 8)	3.1%
0.5% EDTA 3% NH_4OH	0.30 (0.02, n = 9)	7.9%	0.42 (0.02, n = 8)	4.2%	1.00 (0.05, n = 8)	4.9%	3.86 (0.16, n = 8)	4.1%
1% EDTA 3% NH_4OH	0.28 (0.03, n = 9)	9.3%	0.39 (0.02, n = 8)	4.8%	0.93 (0.04, n = 8)	4.1%	3.83 (0.07, n = 8)	1.7%
3% EDTA 3% NH_4OH	0.30 (0.01, n = 9)	4.7%	0.43 (0.02, n = 8)	3.7%	0.98 (0.02, n = 8)	2.3%	3.94 (0.08, n = 8)	2.1%

3.2. *Effect of leaching time*

Under typical carbonate leaching conditions (i.e., 3% HNO_3), the reaction of different iodine species will lead to the formation of volatile I_2 and/or HOI species (e.g., Cook et al., 2022). It is thus conceivable that excessive leaching time may result in iodine loss from leachates. Although the issue has been recognised (e.g., He et al., 2022; Huang et al., 2022; Cook et al., 2022), few studies have explicitly sought to characterise iodine loss over time during leaching of carbonate rocks. Our comparative trials show no significant iodine loss during sample dissolution for limestones and dolostones when the leaching time is within 60 min (Fig. S2). Although there is a slight tendency toward lower values in C32.6 and C31, the differences are mostly within 5%, which is acceptable considering typical analytical errors and sample heterogeneity. The most striking drop is observed in all samples when the leaching time extends to 120 min, with I/(Ca + Mg) lower by 49% on average (Fig. S2).

The iodine derived from carbonate leaching should be dominated by the non-volatile IO_3^- (Lu et al., 2010; Hashim et al., 2022). Transformation of IO_3^- to easily volatile I_2 or less volatile HOI involves the formation of intermediate species (e.g., HIO_3 and I_2O_2) and requires I^- oxidation (reactions 1–5; Furuichi and Liebhafsky, 1975; Xie et al., 1999; Schmitz, 2000). Given the possibly very low I^- concentration in leachates, we consider that the relative iodine stability in the first hour of leaching is because iodine volatilization may be kinetically limited. On the other hand, prolonged ultrasonication would inevitably increase

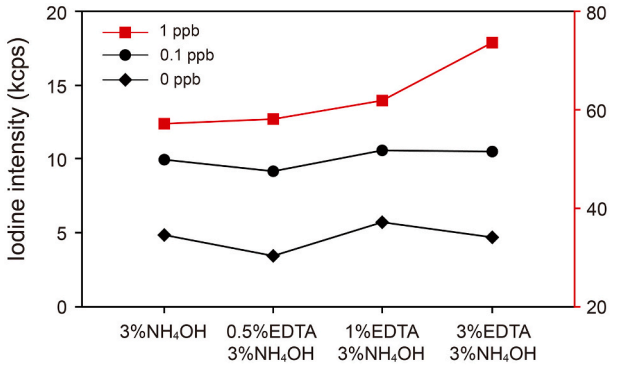

Fig. 2. Iodine intensities of different concentration calibration standards in different matrixes. Note that iodine intensities for the 1 ppb standard solutions correspond to the right y-axis.

the water temperature, which may play a role in iodine loss between 60 and 120 min.

$$IO_3^- + H^+ \rightleftharpoons HIO_3 \quad (1)$$

$$HIO_3 + I^- + H^+ \rightleftharpoons I_2O_2 + H_2O \quad (2)$$

$$I_2O_2 + I^- \longrightarrow I_2 + IO_2^- \quad (3)$$

$$I_2O_2 + H_2O \longrightarrow HIO_2 + HOI \quad (4)$$

$$HOI + I^- + H^+ \longrightarrow I_2 + H_2O \quad (5)$$

The leaching times of existing studies vary from 10 min (Hardisty et al., 2017) to overnight (Loope et al., 2013), while most studies keep leaching times within 60 min. Combined with our results, this suggests that most published data obtained under similar typical carbonate leaching conditions are largely comparable. However, we also note that the iodine loss efficiency observed in our study differs from that of Cook et al. (2022), who found significant iodine loss 30 min after foraminifera leaching. Although the mechanism behind the difference remains unclear and certainly deserves further study, we suspect that it might relate to mineralogy (biogenic vs. abiogenic) and solid/liquid ratio. As indicated by reaction equations, the iodine volatilization rate during leaching is also affected by I^- and H^+ concentrations (Furuichi and Liebhafsky, 1975). This implies that iodine stability during leaching might also vary with sample purity and acid strength, which warrants further investigation. We thus suggest that a test for iodine loss be performed if leaching conditions vary significantly.

3.3. *Effect of oxidative cleaning*

Since organic material is typically enriched in iodine (e.g., Muramatsu and Hans Wedepohl, 1998), an inadvertent attack on organic matter during leaching may result in elevated CAI contents. Recently, Glock et al. (2019) and Winkelbauer et al. (2021) showed that benthic and planktic foraminiferal I/Ca ratios can be overestimated without oxidative cleaning. The extent to which oxidative cleaning may affect iodine concentrations in ancient carbonates remains unexplored. Therefore, we assessed this on organic-rich dolostones from the Gaoyuzhuang Formation by cleaning samples with NaClO and/or H_2O_2 prior to leaching, both of which are commonly used reagents to remove organic matter (e.g., Barker et al., 2003; Wotte et al., 2012).

The samples that were cleaned only with DI water yielded high I/(Ca + Mg) ratios with a mean of 2.16 μmol/mol (Fig. 3). Mean I/(Ca + Mg) ratios for samples cleaned with buffered 1% H_2O_2 (unheated) exhibit little difference from samples cleaned with DI water (Fig. S3). The inefficacy of buffered 1% H_2O_2 in our study may thus support the importance of heating as a normal procedure (e.g., Barker et al., 2003; Lu et al., 2016). By contrast, the measured I/(Ca + Mg) ratios of samples bleached with 12% NaClO are significantly lower than those cleaned with DI water (Fig. 3). The most prominent reduction of I/(Ca + Mg) occurred after the first oxidative cleaning, with the mean value decreased by 31% to 1.50 μmol/mol. Further oxidative cleaning showed only a minor effect on I/(Ca + Mg), resulting in a mean ratio of 1.49 μmol/mol (Fig. 3). Measured I/(Ca + Mg) ratios of pure limestone samples are indistinguishable whether cleaned or uncleaned (Figs. 3, S3).

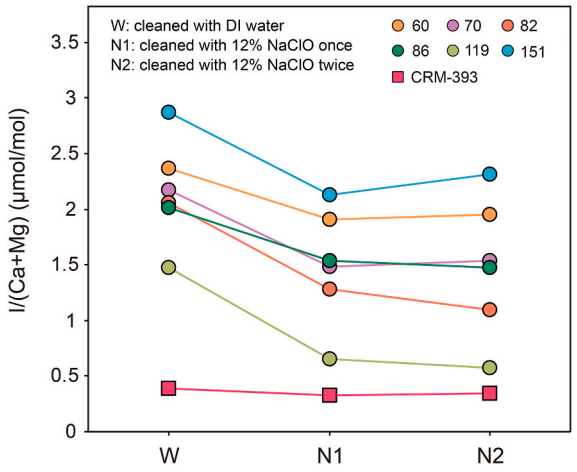

Fig. 3. Comparison of I/(Ca + Mg) values with different cleaning methods for impure organic-rich dolostones (circle) from the Gaoyuzhuang Formation and a pure carbonate standard (square; limestone CRM-393).

Despite the overall difference, one may notice that there are also some subtle differences between leachates. For example, N2 can be slightly higher than N1 (Fig. 3), while W can be slightly lower than the same samples cleaned with buffered 1% H_2O_2 (Fig. S3). The cleaned samples were forcibly rinsed with DI water (see Methods), which would inevitably result in the loss of some material. This might have contributed to the slight difference in I/(Ca + Mg). Additionally, since the results were obtained from different independent batches (see Methods), it is conceivable that analytical errors and sample heterogeneity, especially for these organic-rich impure dolostones, could have given rise to the small variability in CAI contents. From a practical perspective, it is usually a dramatic stratigraphic change in CAI contents that pertains to perturbations in the seawater iodate reservoir. Therefore, we focus on the significant change of I/(Ca + Mg) ratios here and regard minor variations as due to internal uncertainty during the whole process.

The most interesting observation is the elevated I/(Ca + Mg) values in uncleaned samples compared with samples cleaned with NaClO (Fig. 3). Theoretically, since the CAI content is expressed as the I/(Ca + Mg) ratio, additional contributions of Ca and/or Mg from contaminants (e.g., from reagents) could possibly produce lower I/(Ca + Mg) values. However, this is an unlikely explanation for the difference between our sample set for two reasons. First, the residues bleached with pure reagent were further rinsed with DI water violently three times (see Methods), which should have removed the reagent. Second, the dissolved carbonate percentages that are calculated from measured Ca and Mg in stock solutions are almost the same in uncleaned samples and samples bleached with NaClO, suggesting negligible addition of Ca and/or Mg from the reagent. These lines of evidence lead us to consider that the elevated I/(Ca + Mg) values in uncleaned samples are possibly due to partial attack of organic matter despite the short leaching time (15 min) and diluted nitric acid, as with modern foraminifera (e.g., Glock et al., 2019; Winkelbauer et al., 2021).

We note that the generality of organic matter contamination remains to be demonstrated as at present too few studies have investigated this aspect. Previous studies have invoked the relationship between I/(Ca +

Mg) and TOC to recognize the potential influence of organic matter (e.g., Shang et al., 2019; Huang et al., 2022), and a positive covariation would be expected if there is a significant contribution from organic matter. However, this is not observed in our sample set despite the presence of organic matter contamination (Fig. 4), implying that such a cross plot may not always be helpful. Instead, we propose that the most efficient way to discern the contribution from organic matter would perhaps be to conduct comparative tests (i.e., oxidatively cleaned vs. uncleaned) for several organic-rich samples in a sample set. This is especially crucial when a prominent increase of I/(Ca + Mg) is interpreted quantitatively since the absolute values may decrease after cleaning (Fig. 4). Overall, as a proof-of-concept, our findings serve as a cautionary tale in that the possibility of organic matter contamination should not be dismissed when working on organic-rich samples.

3.4. Comparison of acid strength and contaminant mixing experiments

It is necessary to ensure that the extracted iodine concentrations from carbonate rocks reflect CAI only since the leaching of non-carbonate phases could mask the primary signals. In addition to organic matter, other possible contaminants include Fe/Mn oxides, phosphates, and silicate minerals. Although the influence of Mn oxide is considered negligible (Zhou et al., 2014), the potential effects of other contaminants, especially phosphates, have not been fully evaluated. Phosphate minerals such as apatites are tolerant to structural distortion and chemical substitution and thus are diverse in molecular composition (Pan and Fleet, 2002). It has been shown that iodates can substitute for hydroxyls in the hydroxyapatite lattices despite the difference in the geometry of both anions (Campayo et al., 2011; Laurencin et al., 2014). Both CO_3^{2-} and SO_4^{2-} ions can be incorporated into apatite crystals during precipitation, while Podder et al. (2017) and Tokunaga et al. (2021) showed that IO_3^- can substitute for CO_3^{2-} and SO_4^{2-} in calcite and barite, respectively, due in part to their similar bond lengths (1.8 Å for I–O, 1.5 Å for S–O, 1.3 Å for C–O). Consequently, iodate ions might replace these ions and even PO_4^{3-} in apatites as well. Francolite (or carbonate fluorapatite) contains abundant F^- which can also be substituted by I^- (Pan and Fleet, 2002). Taken together, it is plausible to assume that phosphates are an important iodine host phase in sedimentary rocks. Indeed, phosphorites from the Doushantuo Formation at Xiaoba section near Weng'an in South China exhibit considerable iodine enrichment with concentrations as high as 98 ppm (Ren et al., 2015). Therefore, inadvertent leaching of phosphates during acid leaching may lead to an overestimation of measured CAI.

The phosphate rock standard SRM-120b leached with 3% HNO_3 gives a high I/(Ca + Mg) ratio of 34.71 μmol/mol consistent with iodine enrichment in the phosphorite. The shale standard SGR-1 instead shows

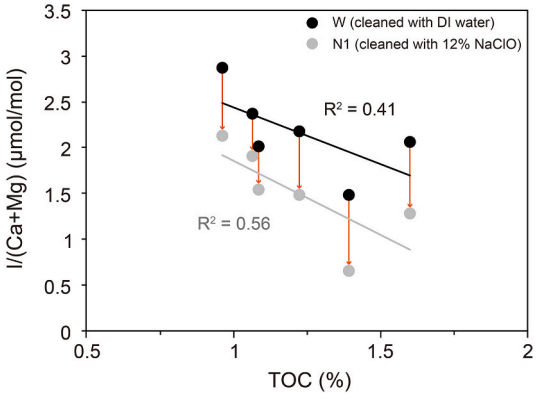

Fig. 4. Cross plot of I/(Ca + Mg) against TOC for impure dolostone duplicates from the Gaoyuzhuang Formation. The I/(Ca + Mg) values are from the previous oxidative cleaning test (Fig. 3).

iodine concentration below the detection limit but has detectable dissolved Ca and Mg contents. This is consistent with the result of Muramatsu and Hans Wedepohl (1998) who reported that the bulk rock iodine content of shale SGR-1 is low at around 334 ppb. When the mixtures of phosphorite SRM-120b and carbonate standards are leached with 3% HNO_3, I/(Ca + Mg) values increase from 3.87 to 14.01 μmol/mol for coral JCp-1, from 0.40 to 10.67 μmol/mol for limestone CRM-393, and from 0.96 to 13.98 μmol/mol for argillaceous limestone SRM-1c (Fig. 5). The dramatically elevated I/(Ca + Mg) in artificial standard mixtures is largely comparable with expected values assuming the complete dissolution of phosphates. This implies that 3% HNO_3 leaching can overestimate CAI concentrations if phosphates are present. Surprisingly, the I/(Ca + Mg) values of mixtures of shale SGR-1 and carbonate standards are close to or slightly lower than that of unmixed carbonate standards (overall ~5% difference). Given the detectable Ca and Mg in the nitric acid leachate of shale SGR-1, the slight reduction of I/(Ca + Mg) in the mixtures is likely to be because SGR-1 released negligible iodine but a small amount of Ca and Mg during 3% HNO_3 leaching.

Although phosphorite SRM-120b yields a similarly high I/(Ca + Mg) ratio of 38.35 μmol/mol when leached with 0.3 M acetic acid, the total dissolved iodine (expressed as dissolved iodine relative to sample weight) is 4.91 μg/g, which is much smaller than that dissolved in 3% HNO_3 (41.53 μg/g). The iodine in the acetic acid leachate of shale SGR-1 is again below the detection limit. The unmixed carbonate standards leached with 0.3 M acetic acid exhibit no significant difference in I/(Ca + Mg) values from those leached with 3% HNO_3 (Fig. 5). Their I/(Ca + Mg) values are also not significantly different from (though slightly higher than) those of mixtures of carbonate standards with shale SGR-1 (Fig. 5) under acetic acid leaching, similar to what has been observed in nitric acid leaching (Fig. 5). Considering that silicate minerals constitute the primary component of shale SGR-1, the little iodine released from the leaching of SGR-1 implies that silicate minerals are perhaps not a significant source of iodine contamination in carbonate rocks. In contrast, for the mixtures of carbonate standards with phosphorite SRM-120b, the I/(Ca + Mg) values in acetic acid leachates are several times to an order of magnitude lower than the expected values under the assumption of the complete dissolution of phosphates, and also are much lower than those from nitric acid leachates (Fig. 5). Together with lower dissolved iodine in the acetic acid leachate of phosphorite SRM-120b, it indicates that 0.3 M acetic acid leaching can effectively reduce phosphate dissolution.

The standard mixing experiments support the idea that phosphate minerals are an important iodine-bearing phase and could be a potential contaminant for the CAI analysis. Nevertheless, it should be noted that the extent of contamination, as indicated in our study (i.e., one order of magnitude higher), is likely to be an extreme case considering the high mixing ratio (>20%). The content of phosphate minerals in geological carbonate samples is generally lower. Since phosphate minerals are most likely dispersed in the matrix of geological carbonate samples (e.g., Sanders and Grotzinger, 2021), their active surface area is also likely decreased compared with the simple standard mixing. Collectively, it is reasonable to presume that the effect of phosphate contamination by 3% HNO_3 or 0.3 M acetic acid leaching would be reduced in geological samples. Conversely, it has been demonstrated that dilute nitric acid can dissolve phosphates in geological samples (e.g., Li et al., 2011), and hence, even if the severity of phosphate contamination were reduced in geological samples, it is still important to consider its influence especially when phosphate minerals are present. On the other hand, the phosphate dissolution is already diminished by 0.3 M acetic acid leaching in the case of simple standard mixing (Fig. 5). A similar strength of acetic acid (0.33 M) has also been preferred to extract carbonate-associated phosphorus to avoid leaching apatite (e.g., Ingalls et al., 2022). Together, we suggest that 0.3 M acetic acid leaching is a reliable means to mitigate the influence of phosphate contamination, if any.

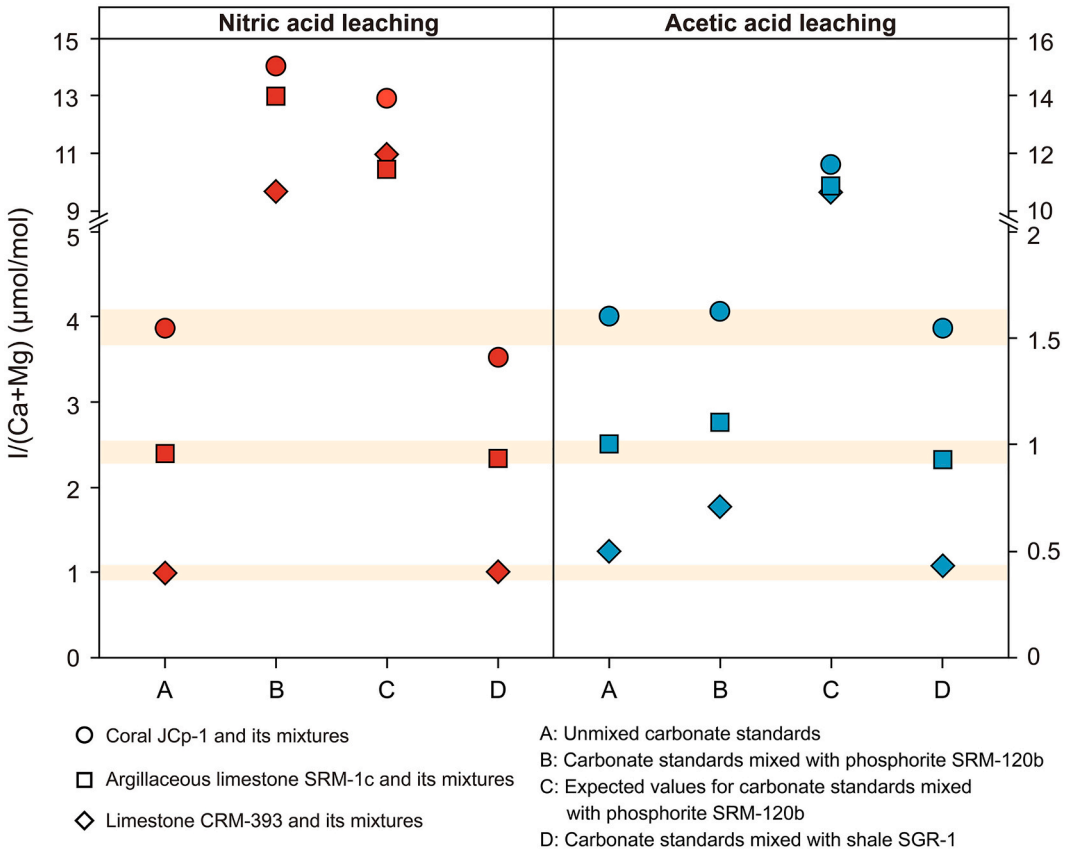

Fig. 5. Comparison of I/(Ca + Mg) values for standards and artificial standard mixtures leached with 3% HNO_3 (red; left) and 0.3 M acetic acid (blue; right). The leaching process is the same as the common practice (see Methods for details). Faint colour bands show the range of ±5% deviation from the unmixed standard I/(Ca + Mg) values leached with 3% HNO_3. The expected I/(Ca + Mg) values are calculated by assuming the complete dissolution of the phosphorite SRM-120b. The mixing ratios range from 21% to 24% for the shale and 21–35% for the phosphate rock. Note that values for limestone CRM-393, argillaceous limestone SRM-1c and their mixtures correspond to the y-axis on the right. (For interpretation of the references to colour in this figure legend, the reader is referred to the web version of this article.)

The iodine concentrations of dolostone samples from the Gaoyuzhuang and Tieling formations leached with different acids are shown in Fig. 6. For the relatively pure dolostones, there are no significant differences in I/(Ca + Mg) values between samples leached with 3% HNO_3 and 0.3 M acetic acid (Fig. 6). By contrast, the I/(Ca + Mg) decreases by on average 17% for most impure dolostones, except for samples 119 and 151 from the Gaoyuzhuang Formation whose I/(Ca + Mg) ratios are elevated in acetic acid leachates (Fig. 6). There are two possible explanations for the I/(Ca + Mg) differences between nitric and acetic acid leachates of dolostones. The first contributing factor should come from the difference in the dissolved carbonate phase. Under the condition of the same leaching time and acid volume, acetic acid dissolves less carbonate than nitric acid, and in our case, an average of 95% of the carbonate was dissolved by 3% HNO_3, whereas the ratio was only 59% for acetic acid. As revealed in the following section, different carbonate phases could have different iodine concentrations, similar to what has been discovered for REE and Sr isotopes in carbonate rocks (e.g., Bailey et al., 2000; Tostevin et al., 2016). Therefore, the increase of I/(Ca + Mg) in acetic acid leachates (e.g., sample 151) could be attributed to high I/(Ca + Mg) in the dissolved carbonates (Fig. 7). In this regard, the similar I/(Ca + Mg) values in nitric and acetic acid leachates of pure dolostones are likely to be because the dissolved carbonate phases contain relatively consistent iodine concentrations (Fig. 7).

The second contributing factor may pertain to the use of a weak acid. The impure dolostones from member III of the Gaoyuzhuang Formation have been demonstrated to be relatively enriched in organic matter and phosphate minerals (Shang et al., 2019). The lower I/(Ca + Mg) values in these acetic acid leachates (Fig. 6) may thus represent decreased

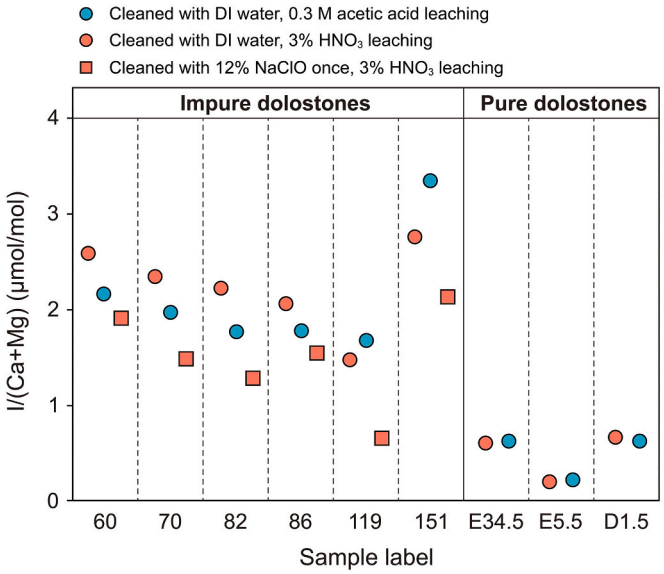

Fig. 6. Comparison of I/(Ca + Mg) values for impure and pure dolostones leached with 3% HNO_3 (red) and 0.3 M acetic acid (blue). Squares represent sample values obtained by pre-cleaning with 12% NaClO once (N1) in the previous experiment (Fig. 3). (For interpretation of the references to colour in this figure legend, the reader is referred to the web version of this article.)

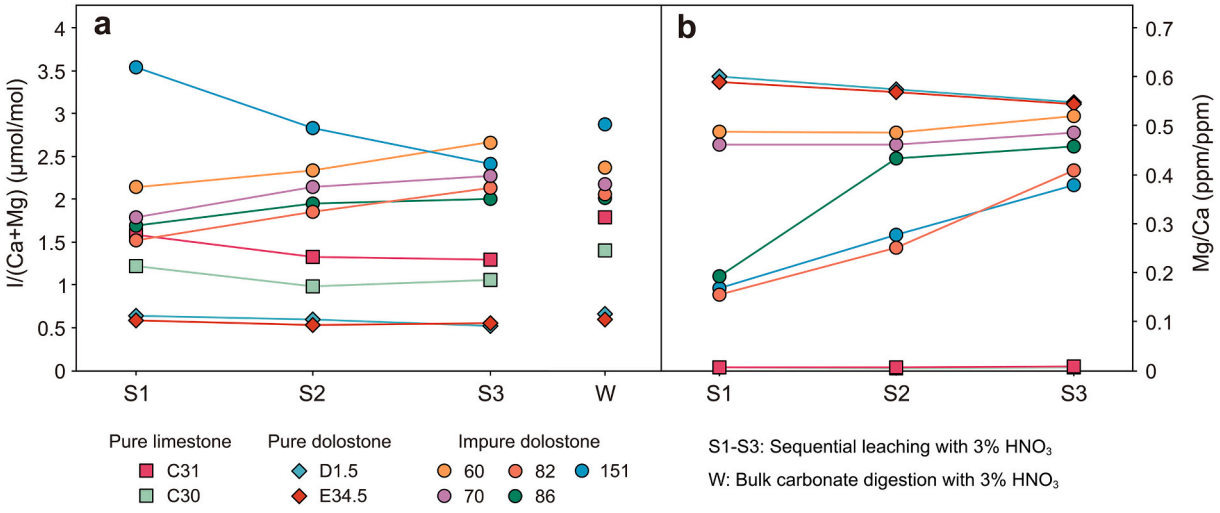

Fig. 7. Sequential leaching results of (a) I/(Ca + Mg) and (b) Mg/Ca ratios in carbonate rocks from the Gaoyuzhuang and Tieling formations. W represents I/(Ca + Mg) values obtained by bulk carbonate digestion in the previous experiments prewashed with DI water only (Fig. S2 and Fig. 3). Note that the symbols for Mg/Ca ratios of C31 and C30 overlap.

contamination of the aforementioned non-carbonate phases. However, the lower I/(Ca + Mg) values are also comparable to those from the first sequential leachates (S1 in Fig. 7), although we note that the dissolved carbonate contents are not necessarily the same. This may imply that the phosphate contamination could be decreased during sequential leaching perhaps due to the absence of excess acid. Alternatively, this may also reflect that, combined with the reduced reactivity of phosphate minerals in real samples, their contents in studied samples are probably not high enough to induce a significant impact. Clearly, the potential significance of phosphate contamination warrants further investigation. Nonetheless, we note that for impure dolostones, the I/(Ca + Mg) values obtained by 0.3 M acetic acid leaching are still higher than that obtained with oxidative cleaning (Fig. 6), further illustrating the importance of oxidative cleaning for iodine analysis in organic-rich carbonate rocks.

3.5. Sequential leaching

Sequential leaching is a technique initially developed to isolate different phases in rocks and consequently provide insights into the partitioning of elements among phases (Tessier et al., 1979). It has been applied to extract the least contaminated or altered carbonate Sr, U, and Ba isotopes, and REE (e.g., Bailey et al., 2000; Li et al., 2011; Tostevin et al., 2016; Dahl et al., 2019; Lin et al., 2020; Chen and Zhou, 2023). However, whether sequentially leached carbonate phases exhibit different iodine contents has yet to be fully assessed, and so we expand on this here. As shown in Fig. 7, the I/(Ca + Mg) values are consistently highest in the first leachates for relatively pure limestones and dolostones, before decreasing slightly in the subsequent leachates. Conversely, the first leachates have the lowest I/(Ca + Mg) values for most impure dolostones, with I/(Ca + Mg) gradually increasing in the successive leachates. The impure dolostone 151 is unusual in that the earlier dissolved carbonates contain relatively high I/(Ca + Mg) (Fig. 7). Given that acetic acid may only dissolve carbonates partially, our sequential leaching results here support the inference above that the elevated I/(Ca + Mg) in the acetic acid leachate of dolostone 151 (Fig. 6) is due in part to high I/(Ca + Mg) in the dissolved carbonates.

The Mg/Ca ratio of the dissolved carbonates also varies during sequential leaching, exhibiting slight variations for limestones and highly dolomitised carbonate rocks and a gradually increasing trend for partially dolomitised carbonate rocks (Fig. 7). This increasing trend is consistent with previous sequential leaching studies of dolomitic limestones, and has been attributed to the faster kinetics of calcite relative to dolomite dissolution (Chou et al., 1989; Tostevin et al., 2016). We note that this does not necessarily imply that calcite retains the primary CAI signal as it can also precipitate during diagenetic processes. More recently, Tang et al. (2023) argue that I/(Ca + Mg) in calcite and dolomite of a bulk rock could reflect different redox conditions of ambient fluids during precipitation. In their case, the low I/(Ca + Mg) in calcite is considered to reflect precipitation in shallow suboxic porewater, whereas dolomite with relatively high I/(Ca + Mg) is interpreted to form in more oxidised porewater. Likewise, the varying I/(Ca + Mg) in our sequentially dissolved carbonates may reflect different redox conditions of their different precipitation loci (e.g., water column, sediment-water interface, or porewater). On the other hand, it is commonly accepted that diagenetic alteration, including dolomitization, tends to decrease CAI concentrations (Loope et al., 2013; Hardisty et al., 2017), which is possibly related to the relatively lower partition coefficient of iodate in dolomite than calcite (Hashim et al., 2022). Therefore, the I/(Ca + Mg) may also decrease to varying extents with increasing dolomitization.

Both mechanisms could have played a role in shaping I/(Ca + Mg) of different carbonate phases and different carbonate phases may have been dissolved during sequential leaching. Given the uncertainty, we acknowledge that the exact reasons for varying I/(Ca + Mg) concentrations with sequential leaching warrant further study. Still, there are two important implications from our results. First, the consistently high I/(Ca + Mg) in highly dolomitised Tieling samples (Fig. 7) reinforces the notion that some Precambrian dolostone can probably record primary seawater signals on account of precipitation near the sediment-water interface (Hardisty et al., 2017). Second, the bulk carbonate I/(Ca + Mg) values of impure dolostones are lower than or close to those of sequentially leached carbonate phases (Fig. 7). This is because the bulk carbonate I/(Ca + Mg) reflects the weighted average of different carbonate phases and diagenetic (and/or authigenic) carbonates generally contain lower I/(Ca + Mg) values (Lu et al., 2020b; Lau and Hardisty, 2022; Hashim et al., 2022; Tang et al., 2023). Accordingly, the I/(Ca + Mg) obtained from bulk carbonate digestion could potentially be reduced from primary values due to the presence of diagenetic (and/or authigenic) carbonate phases. This implies that the bulk carbonate I/(Ca + Mg) has the potential to result in underestimation of the (minimum) size of the local-regional seawater IO_3^- reservoir.

3.6. Recommended leaching strategy and alternative rock standards

Our findings indicate that oxidative cleaning by 12% NaClO has a significant impact on the CAI concentrations of impure organic-rich carbonate rocks, while it has little effect on relatively pure carbonate rocks (Fig. 3). Phosphate minerals, if present in abundance, should also be considered as a potential contaminant that can be mitigated through the use of 0.3 M acetic acid for leaching (Fig. 5). While 0.3 M acetic acid is suitable for dissolving impure carbonate rocks, it may be not necessary for relatively pure carbonate rocks (Figs. 5 and 6). Combined with these observations, we propose a leaching procedure to extract carbonate-associated iodine from relatively pure and impure organic-rich carbonate rocks (Fig. 8). Nevertheless, we note that this is a general guide only and several aspects could be adjusted when applied to specific samples. For example, although we demonstrated that iodine is relatively stable for 60 min in the acidic solution during a typical leaching process (Fig. S2), the stability could vary with sample purity, acid strength and volume. Consequently, the leaching time is kept within 15–30 min in the protocol as a precaution, unless tests have been conducted to assess the likely extent of iodine loss under other leaching conditions. As discussed previously (Sections 3.3 and 3.4), the generality of organic matter and/or phosphate contamination also warrants further study, while the recommended screening cut-off is related to the properties of our specific sample set. As such, instead of directly applying the proposed threshold, we strongly suggest that for an organic-rich sample set, a preliminary test on several samples is conducted to assess the potential contribution from organic matter and/or phosphate minerals. With increasing data in future, the geochemistry community might ultimately have the capability to set robust thresholds. Moreover, carbonate mineralogy also likely influences the leaching strategy. This is because acetic acid preferentially dissolves calcite rather than dolomite. Accordingly, the intention to obtain bulk I/(Ca + Mg) from dolostones or dolomitised carbonate rocks may have to be compromised if there are concomitant contaminants. In this case, sequential leaching with acetic acid provides a possible means to roughly obtain bulk carbonate I/(Ca + Mg) values. Certainly, additional studies would be helpful to further optimise the leaching strategies. Overall, our study highlights that the possibility for contamination during leaching should not be dismissed, and that leaching strategies can be adjusted depending on sample purity and mineralogy.

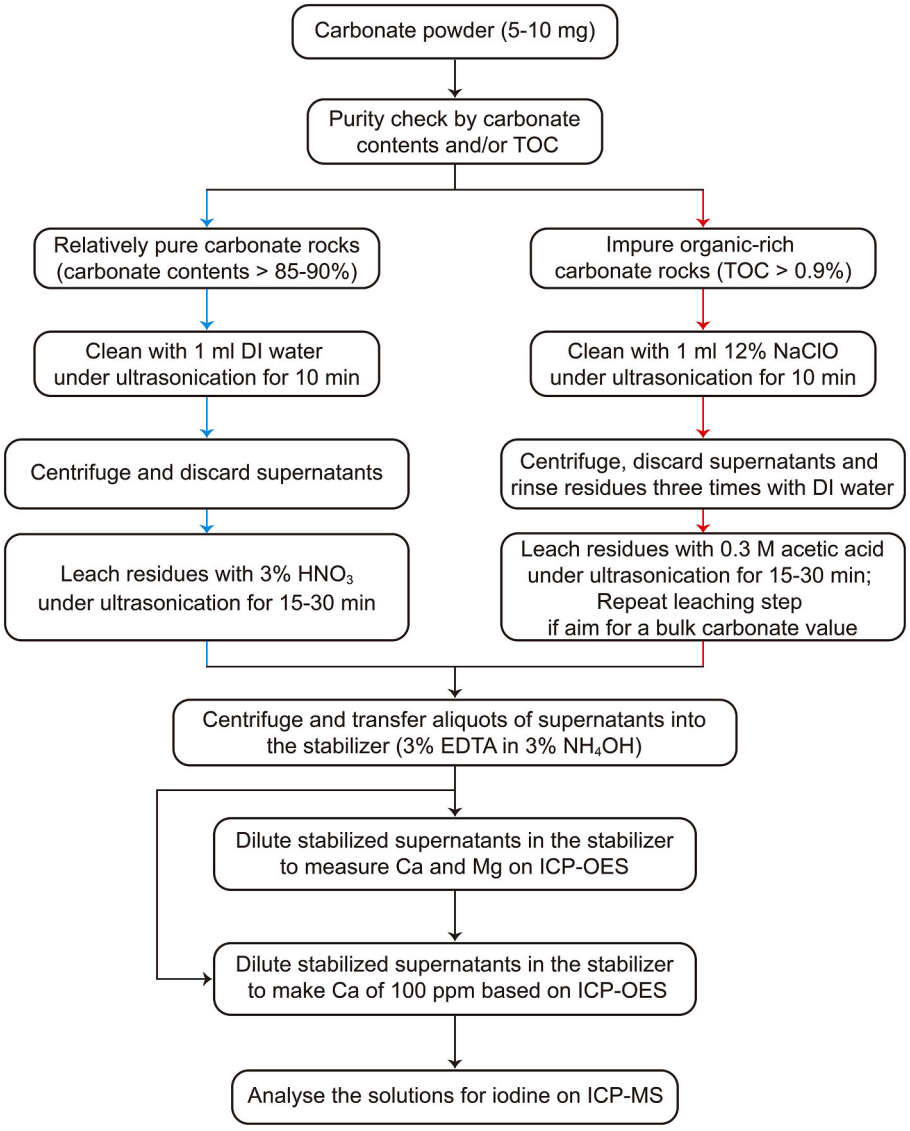

Fig. 8. Proposed leaching procedure for extracting carbonate-associated iodine in relatively pure and impure organic-rich carbonate rocks. Note that this is a general guide only and the screening cut-off could be different between sample sets. Acid volumes and leaching times may vary with sample purity and mineralogy and could be assessed with a preliminary test.

The most commonly used reference material for quality control of iodine data is coral JCp-1, but unfortunately, it is not easily accessible now (Lu et al., 2020b). Its utility is also plagued by the substantial variability of reported values in the literature. For example, earlier analyses of coral JCp-1 yielded relatively high I/Ca of 4.33 ± 0.36 μmol/mol (Chai and Muramatsu, 2007) and 4.27 ± 0.06 μmol/mol (Lu et al., 2010), but relatively low values of 3.82 ± 0.39 μmol/mol (Glock et al., 2014) and 3.70 ± 0.27 μmol/mol (Lu et al., 2020b) have also been reported. More recently, Winkelbauer et al. (2021) and He et al. (2022) reported slightly higher I/Ca values of 4.53 ± 0.11 μmol/mol and 4.52 ± 0.14 μmol/mol, respectively. The differences have been attributed to iodine heterogeneity in coral JCp-1 (Winkelbauer et al., 2021). Importantly, the range of I/Ca ratios in JCp-1 exceeds absolute sample iodine concentrations in some cases, which causes considerable uncertainty when comparing results from carbonate rocks with relatively low iodine contents (e.g., Precambrian carbonate rocks). Therefore, more easily accessible reference materials with homogeneous iodine concentrations would be desirable. Lu et al. (2020b) proposed using synthetic calcite with I/Ca of 3.52 ± 0.27 μmol/mol as an alternative, but this is not yet widely available. As mentioned previously, we unexpectedly found two promising limestone reference materials, i.e., limestone CRM-393 and argillaceous limestone SRM-1c, during optimisation of the stabilizer. Their CAI contents are relatively low but well in the range of most Precambrian carbonate rocks. Therefore, we measured the two reference materials multiple times during the measurement period (one year). We compiled the measured values (Fig. 9), which were obtained by dissolving standards in 3% HNO_3 directly, followed by stabilization in 3% NH_4OH with EDTA. Long-term measurements of the duplicates show relatively stable values with I/Ca of 0.43 ± 0.03 μmol/mol (1SD, n = 14) for limestone CRM-393 and 0.99 ± 0.06 μmol/mol (1SD, n = 14) for argillaceous limestone SRM-1c (Fig. 9). The relatively low I/Ca values of the limestone standards make them particularly useful for assessing CAI data of Precambrian carbonate rocks. We thus recommend that the two reference materials can be used as complementary interlaboratory standards for iodine analysis.

4. Implications for carbonate-associated iodine as a redox proxy

The CAI proxy has been widely used to infer paleoredox conditions related to biological evolution, mass extinction, and oceanic anoxic events (e.g., Lu et al., 2010; Hardisty et al., 2014; Lu et al., 2018; Edwards et al., 2018; He et al., 2022). One of the advantages of the proxy is that diagenetic processes generally lead to iodine loss from carbonate rocks (Hardisty et al., 2017). The bulk carbonate iodine concentrations are thus commonly considered to place constraints on minimum regional IO_3^- availability, which is potentially linked to dissolved oxygen levels (e.g., Lu et al., 2016; Lu et al., 2018). However, similarly strong acid leaching has been equally applied to ancient carbonate rocks even though carbonate purities can vary significantly, and hence, it remains uncertain whether some published data reflect true CAI values. Our results demonstrate that CAI can be underestimated by as much as 49% on average during carbonate leaching due to prolonged exposure (>60 min) of iodine in a 3% HNO_3 solution (Fig. S2). However, we reiterate that the iodine stability varies with acid strength and I^- concentration in solution, and a preliminary test is recommended when leaching conditions vary significantly from the standard. Bulk carbonate I/(Ca + Mg) values can also be lowered (up to 18% in the case of our study) by the presence of diagenetic (and/or authigenic) carbonate phases (Fig. 7). It is thus plausible that some relatively high I/(Ca + Mg) values might be masked due to bulk carbonate leaching, depending on the proportion of diagenetic carbonates, which would further underestimate the minimum iodate availability. Furthermore, our data also suggest that non-carbonate phases such as organic matter and phosphate minerals should be regarded as potential contaminants, the inadvertent leaching of which could lead to overestimated I/(Ca + Mg) values. Given these observations, the coupled variation of I/(Ca + Mg) and lithology (such as increasing iodine concentrations with increasing muddy or phosphate contents) throughout the stratigraphic column should be treated cautiously. For future studies on iodine contents of impure carbonate rocks, we strongly suggest that a preliminary test of several samples on the effects of non-carbonate phase contamination is of great importance, and our leaching strategy offers a way to minimise the contaminations. Additionally, for the (semi-)quantitative application of the CAI proxy, the I/Ca threshold of ~2.5–3.0 μmol/mol in foraminifera has been proposed to indicate hypoxic seawater (O_2 < ~20–70 μM) in near-modern conditions (Lu et al., 2016; Lu et al., 2022). This threshold has also been invoked to infer oxygen levels in deep time. However, as shown in Fig. 4, the bulk carbonate I/(Ca + Mg) values in oxidatively cleaned samples can be lowered from above to below the threshold. Therefore, although organic matter cleaning may not significantly affect the qualitative interpretation of stratigraphic CAI trends, quantitative interpretation of bulk carbonate I/(Ca + Mg) in deep time studies (i.e., inference of dissolved oxygen levels) should still be treated with caution.

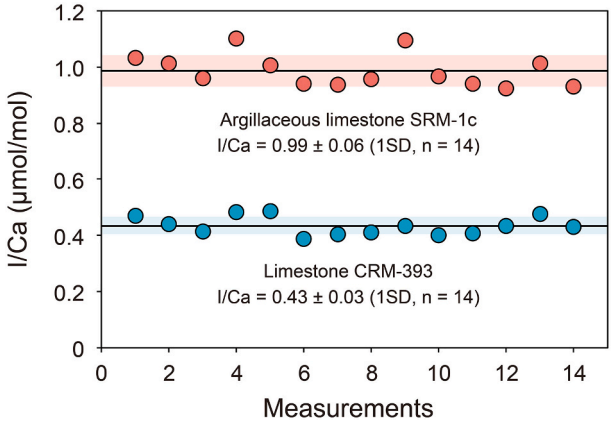

Fig. 9. Long-term measurements (one year) of I/Ca values in different batches for standard duplicates of limestone CRM-393 (blue) and argillaceous limestone SRM-1c (red). Solid black lines indicate the average values and faint colour bands show the range of one standard deviation. (For interpretation of the references to colour in this figure legend, the reader is referred to the web version of this article.)

5. Conclusions

Our results indicate that NaOH or NH_4OH alone may not be ideal reagents for iodine analysis for carbonate-associated iodine (CAI) studies. Instead, a mixture of 3% EDTA and 3% NH_4OH stabilizes iodine well and prevents the precipitation of calcium and magnesium ions from the alkaline solution. This advantage can ease the preparation process and reduce signal drift during CAI analysis, making the new reagent a useful supplement to existing stabilizers. Our leaching experiments demonstrate that iodine is relatively stable in acidic solutions for ~60 min, but nearly half of the iodine can be lost under prolonged acid leaching. The results support that iodine data obtained under similar typical leaching conditions are largely comparable. Future studies are required, however, to better understand iodine stability behaviour under different leaching conditions. Comparison of CAI concentrations in sequentially leached carbonate phases suggests that the dissolution of diagenetic (and/or authigenic) carbonates could lower bulk carbonate iodine concentrations. The maximum dilution of CAI is 18% in our study, but could be even higher depending on the proportion of diagenetic (and/or authigenic) carbonates. On the other hand, we show that organic matter and phosphate contamination can lead to overestimated CAI concentrations. Although the extent of such contamination warrants further study, we show that, if present, oxidative cleaning of 12% NaClO and 0.3 M acetic acid leaching can effectively minimise their contributions, and recommend that this or a similar protocol be applied to at

least several samples for a preliminary test of the effects of contaminations when working on ancient impure carbonate rocks. Finally, we suggest two limestone reference materials (limestone CRM-393 and argillaceous limestone SRM-1c), based on the long-term reproducibility of measured I/Ca values, the suitable value ranges, and accessibility, as potential interlaboratory standards for iodine analysis.

CRediT authorship contribution statement

Kun Zhang: Conceptualization, Investigation, Methodology, Visualization, Writing – original draft, Writing – review & editing. **Gary Tarbuck:** Investigation, Methodology, Resources. **Graham A. Shields:** Conceptualization, Resources, Supervision, Writing – review & editing.

Declaration of Competing Interest

The authors declare that they have no known competing financial interests or personal relationships that could have appeared to influence the work reported in this paper.

Data availability

Data are available through Mendeley Data at https://doi.org/10.17632/t78vh7h5t6.1.

Acknowledgements

This study was financially supported by NERC (NE/R010129/1). KZ acknowledges support from a University College London Faculty Dean's Prize and the China Scholarship Council. We thank Lanyun Miao and Hanqing Zhao for their assistance in field work. We are grateful to Colin Mettam and Xi Chen for providing Gaoyuzhuang samples and TOC data, and Tianchen He and Satoshi Takahashi for providing the reference material JCp-1. We thank Zunli Lu for providing kind suggestions at the initial stage of setting up iodine analysis at UCL. Constructive comments by Zunli Lu and anonymous reviewers improved the manuscript greatly. We are also grateful to Don Porcelli for his editorial handling. For the purpose of open access, the author has applied a Creative Commons Attribution (CC BY) licence to any Author Accepted Manuscript version arising.

Appendix A. Supplementary data

Supplementary data to this article can be found online at https://doi.org/10.1016/j.chemgeo.2023.121896.

References

Agatemor, C., Beauchemin, D., 2011. Matrix effects in inductively coupled plasma mass spectrometry: a review. Anal. Chim. Acta 706, 66–83.
Alcott, L.J., Mills, B.J.W., Poulton, S.W., 2019. Stepwise Earth oxygenation is an inherent property of global biogeochemical cycling. Science 366, 1333–1337.
Andersen, M.B., Romaniello, S., Vance, D., Little, S.H., Herdman, R., Lyons, T.W., 2014. A modern framework for the interpretation of 238U/235U in studies of ancient ocean redox. Earth Planet. Sci. Lett. 400, 184–194.
Ariga, T., Zhu, Y., Inagaki, K., 2019. Study on carbon-induced signal enhancement in inductively coupled plasma mass spectrometry: an approach from the spatial distribution of analyte signal intensities. J. Anal. At. Spectrom. 34, 1865–1874.
Bailey, T.R., McArthur, J.M., Prince, H., Thirlwall, M.F., 2000. Dissolution methods for strontium isotope stratigraphy: whole rock analysis. Chem. Geol. 167, 313–319.
Barker, S., Greaves, M., Elderfield, H., 2003. A study of cleaning procedures used for foraminiferal Mg/Ca paleothermometry. Geochem. Geophys. Geosyst. 4, 1–20.
Bellefroid, E.J., Hood, A.V.S., Hoffman, P.F., Thomas, M.D., Reinhard, C.T., Planavsky, N.J., 2018. Constraints on Paleoproterozoic atmospheric oxygen levels. Proc. Natl. Acad. Sci. 115, 8104–8109.
Broecker, S.W., Peng, T.H., 1982. Tracers in the Sea. Lamont-Doherty Geological Observatory. Columbia University, New York.
Byegård, J., Skarnemark, G., Skålberg, M., 1999. The stability of some metal EDTA, DTPA and DOTA complexes: application as tracers in groundwater studies. J. Radioanal. Nucl. Chem. 241, 281–290.
Campayo, L., Grandjean, A., Coulon, A., Delorme, R., Vantelon, D., Laurencin, D., 2011. Incorporation of iodates into hydroxyapatites: a new approach for the confinement of radioactive iodine. J. Mater. Chem. 21, 17609–17611.
Cao, C., Liu, X.-M., Bataille, C.P., Liu, C., 2020. What do Ce anomalies in marine carbonates really mean? A perspective from leaching experiments. Chem. Geol. 532, 119413.
Cao, C., Liu, X.M., Chen, J., 2022. Cerium anomaly as a tracer for paleo-oceanic redox conditions: a thermodynamics-based Ce oxidation modeling approach. Front. Earth Sci. 10, 1–13.
Chai, J.Y., Muramatsu, Y., 2007. Determination of bromine and iodine in twenty-three geochemical reference materials by ICP-MS. Geostand. Geoanal. Res. 31, 143–150.
Chance, R., Baker, A.R., Carpenter, L., Jickells, T.D., 2014. The distribution of iodide at the sea surface. Environ Sci Process Impacts 16, 1841–1859.
Cheatham, M.M., Sangrey, W.F., White, W.M., 1993. Sources of error in external calibration ICP-MS analysis of geological samples and an improved non-linear drift correction procedure. Spectrochim. Acta Part B At. Spectrosc. 48, 487–506.
Chen, X., Zhou, Y., 2023. Effective leaching of argillaceous and dolomitic carbonate rocks for strontium isotope stratigraphy. Geostand. Geoanal. Res. 1–19.
Chou, L., Garrels, R.M., Wollast, R., 1989. Comparative study of the kinetics and mechanisms of dissolution of carbonate minerals. Chem. Geol. 78, 269–282.
Clarkson, M.O., Poulton, S.W., Guilbaud, R., Wood, R.A., 2014. Assessing the utility of Fe/Al and Fe-speciation to record water column redox conditions in carbonate-rich sediments. Chem. Geol. 382, 111–122.
Cook, M.K., Dial, A.R., Hendy, I.L., 2022. Iodine stability as a function of pH and its implications for simultaneous multi-element ICP-MS analysis of marine carbonates for paleoenvironmental reconstructions. Mar. Chem. 245, 104148.
Cutter, G.A., Moffett, J.G., Nielsdóttir, M.C., Sanial, V., 2018. Multiple oxidation state trace elements in suboxic waters off Peru: in situ redox processes and advective/diffusive horizontal transport. Mar. Chem. 201, 77–89.
Dahl, T.W., Connelly, J.N., Li, D., Kouchinsky, A., Gill, B.C., Porter, S., Maloof, A.C., Bizzarro, M., 2019. Atmosphere-ocean oxygen and productivity dynamics during early animal radiations. Proc. Natl. Acad. Sci. U. S. A. 116, 19352–19361.
De Baar, H.J.W., Bacon, M.P., Brewer, P.G., Bruland, K.W., 1985. Rare earth elements in the Pacific and Atlantic Oceans. Geochim. Cosmochim. Acta 49, 1943–1959.
Edwards, C.T., Fike, D.A., Saltzman, M.R., Lu, W., Lu, Z., 2018. Evidence for local and global redox conditions at an Early Ordovician (Tremadocian) mass extinction. Earth Planet. Sci. Lett. 481, 125–135.
Fakhraee, M., Hancisse, O., Canfield, D.E., Crowe, S.A., Katsev, S., 2019. Proterozoic seawater sulfate scarcity and the evolution of ocean–atmosphere chemistry. Nat. Geosci. 12, 375–380.
Flores, E.M.M., Mello, P.A., Krzyzaniak, S.R., Cauduro, V.H., Picoloto, R.S., 2020. Challenges and trends for halogen determination by inductively coupled plasma mass spectrometry: a review. Rapid Commun. Mass Spectrom. 34.
Furuichi, R., Liebhafsky, H.A., 1975. Rate of the Dushman reaction in iodic acid at low iodide concentration. Complexity of iodic acid. Bull. Chem. Soc. Jpn. 48, 745–750.
German, C.R., Elderfield, H., 1990. Application of the Ce anomaly as a paleoredox indicator: the ground rules. Paleoceanography 5, 823–833.
Glock, N., Liebetrau, V., Eisenhauer, A., 2014. I/Ca ratios in benthic foraminifera from the Peruvian oxygen minimum zone: Analytical methodology and evaluation as a proxy for redox conditions. Biogeosciences 11, 7077–7095.
Glock, N., Liebetrau, V., Vogts, A., Eisenhauer, A., 2019. Organic heterogeneities in foraminiferal calcite traced through the distribution of N, S, and I measured with nanosims: a new challenge for element-ratio-based paleoproxies? Front. Earth Sci. 7, 1–14.
Grindlay, G., Mora, J., De Loos-Vollebregt, M., Vanhaecke, F., 2013. A systematic study on the influence of carbon on the behavior of hard-to-ionize elements in inductively coupled plasma-mass spectrometry. Spectrochim Acta - Part B At. Spectrosc. 86, 42–49.
Hardisty, D.S., Lu, Z., Planavsky, N.J., Bekker, A., Philippot, P., Zhou, X., Lyons, T.W., 2014. An iodine record of Paleoproterozoic surface ocean oxygenation. Geology 42, 619–622.
Hardisty, D.S., Lu, Z., Bekker, A., Diamond, C.W., Gill, B.C., Jiang, G., Kah, L.C., Knoll, A. H., Loyd, S.J., Osburn, M.R., Planavsky, N.J., Wang, C., Zhou, X., Lyons, T.W., 2017. Perspectives on Proterozoic surface ocean redox from iodine contents in ancient and recent carbonate. Earth Planet. Sci. Lett. 463, 159–170.
Hardisty, D.S., Horner, T.J., Evans, N., Moriyasu, R., Babbin, A.R., Wankel, S.D., Moffett, J.W., Nielsen, S.G., 2021. Limited iodate reduction in shipboard seawater incubations from the Eastern Tropical North Pacific oxygen deficient zone. Earth Planet. Sci. Lett. 554, 116676.
Hashim, M.S., Burke, J.E., Hardisty, D.S., Kaczmarek, S.E., 2022. Iodine incorporation into dolomite: experimental constraints and implications for the iodine redox proxy and Proterozoic Ocean. Geochim. Cosmochim. Acta 338, 365–381.
He, T., Zhu, M., Mills, B.J.W., Wynn, P.M., Zhuravlev, A.Y., Tostevin, R., Pogge von Strandmann, P.A.E., Yang, A., Poulton, S.W., Shields, G.A., 2019. Possible links between extreme oxygen perturbations and the Cambrian radiation of animals. Nat. Geosci. 12, 468–474.
He, T., Newton, R.J., Wignall, P.B., Reid, S., Dal Corso, J., Takahashi, S., Wu, H., Todaro, S., Di Stefano, P., Randazzo, V., Rigo, M., Dunhill, A.M., 2022. Shallow Ocean oxygen decline during the end-Triassic mass extinction. Glob. Planet. Chang. 210, 103770.
Huang, K., Cheng, M., Algeo, T.J., Hu, J., Wang, H., Zhang, Z., Dodd, M.S., Wu, Y., Guo, W., Li, C., 2022. Interaction of Shibantan Biota and environment in the terminal Ediacaran Ocean: evidence from I/(Ca+Mg) and sulfur isotopes. Precambrian Res. 379.

Hurtgen, M.T., Arthur, M.A., Suits, N.S., Kaufman, A.J., 2002. The sulfur isotopic composition of Neoproterozoic seawater sulfate: Implications for a snowball Earth? Earth Planet. Sci. Lett. 203, 413–429.
Ingalls, M., Grotzinger, J.P., Present, T., Rasmussen, B., Fischer, W.W., 2022. Carbonate-associated phosphate (CAP) indicates elevated phosphate availability in Neoarchean shallow marine environments. Geophys. Res. Lett. 49.
Kamber, B.S., Webb, G.E., Gallagher, M., 2014. The rare earth element signal in Archaean microbial carbonate: information on ocean redox and biogenicity. J. Geol. Soc. Lond. 171, 745–763.
Kerisit, S.N., Smith, F.N., Saslow, S.A., Hoover, M.E., Lawter, A.R., Qafoku, N.P., 2018. Incorporation modes of iodate in calcite. Environ. Sci. Technol. 52, 5902–5910.
Lau, K.V., Hardisty, D.S., 2022. Modeling the impacts of diagenesis on carbonate paleoredox proxies. Geochim. Cosmochim. Acta 337, 123–139.
Lau, K.V., Maher, K., Altiner, D., Kelley, B.M., Kump, L.R., Lehrmann, D.J., Silva-Tamayo, J.C., Weaver, K.L., Yu, M., Payne, J.L., 2016. Marine anoxia and delayed Earth system recovery after the end-Permian extinction. Proc. Natl. Acad. Sci. U. S. A. 113, 2360–2365.
Laurencin, D., Vantelon, D., Briois, V., Gervais, C., Coulon, A., Grandjean, A., Campayo, L., 2014. Investigation of the local environment of iodate in hydroxyapatite by combination of X-ray absorption spectroscopy and DFT modeling. RSC Adv. 4, 14700–14707.
Lenton, T.M., Boyle, R.A., Poulton, S.W., Shields-Zhou, G.A., Butterfield, N.J., 2014. Co-evolution of eukaryotes and ocean oxygenation in the Neoproterozoic era. Nat. Geosci. 7, 257–265.
Li, D., Shields-Zhou, G.A., Ling, H.F., Thirlwall, M., 2011. Dissolution methods for strontium isotope stratigraphy: guidelines for the use of bulk carbonate and phosphorite rocks. Chem. Geol. 290, 133–144.
Lin, Y.-B., Wei, H.-Z., Jiang, S.-Y., Hohl, S., Lei, H.-L., Liu, X., Dong, G., 2020. Accurate determination of barium isotopic compositions in sequentially leached phases from carbonates by double spike-thermal ionization mass spectrometry (DS-TIMS). Anal. Chem. 92, 2417–2424.
Loope, G.R., Kump, L.R., Arthur, M.A., 2013. Shallow water redox conditions from the Permian-Triassic boundary microbialite: the rare earth element and iodine geochemistry of carbonates from Turkey and South China. Chem. Geol. 351, 195–208.
Lu, Z., Jenkyns, H.C., Rickaby, R.E.M., 2010. Iodine to calcium ratios in marine carbonate as a paleo-redox proxy during oceanic anoxic events. Geology 38, 1107–1110.
Lu, Z., Hoogakker, B.A.A., Hillenbrand, C.-D., Zhou, X., Thomas, E., Gutchess, K.M., Lu, W., Jones, L., Rickaby, R.E.M., 2016. Oxygen depletion recorded in upper waters of the glacial Southern Ocean. Nat. Commun. 7, 11146.
Lu, W., Ridgwell, A., Thomas, E., Hardisty, D.S., Luo, G., Algeo, T.J., Saltzman, M.R., Gill, B.C., Shen, Y., Ling, H.-F., Edwards, C.T., Whalen, M.T., Zhou, X., Gutchess, K. M., Jin, L., Rickaby, R.E.M., Jenkyns, H.C., Lyons, T.W., Lenton, T.M., Kump, L.R., Lu, Z., 2018. Late inception of a resiliently oxygenated upper ocean. Science 177, 174–177.
Lu, W., Dickson, A.J., Thomas, E., Rickaby, R.E.M., Chapman, P., Lu, Z., 2020a. Refining the planktic foraminiferal I/Ca proxy: results from the Southeast Atlantic Ocean. Geochim. Cosmochim. Acta 287, 318–327.
Lu, Z., Lu, W., Rickaby, R.E.M., Thomas, E., 2020b. Earth History of Oxygen and the iprOxy, Earth History of Oxygen and the iprOxy. Cambridge University Press.
Lu, W., Wang, Y., Oppo, D.W., Nielsen, S.G., Costa, K.M., 2022. Comparing paleo-oxygenation proxies (benthic foraminiferal surface porosity, I/Ca, authigenic uranium) on modern sediments and the glacial Arabian Sea. Geochim. Cosmochim. Acta 331, 69–85.
Lyons, T.W., Reinhard, C.T., Planavsky, N.J., 2014. The rise of oxygen in Earth's early ocean and atmosphere. Nature 506, 307–315.
Muramatsu, Y., Hans Wedepohl, K., 1998. The distribution of iodine in the Earth's crust. Chem. Geol. 147, 201–216.
Pan, Y., Fleet, M.E., 2002. Compositions of the apatite-group minerals: substitution mechanisms and controlling factors. Rev. Mineral. Geochem. 48, 13–49.
Podder, J., Lin, J., Sun, W., Botis, S.M., Tse, J., Chen, N., Hu, Y., Li, D., Seaman, J., Pan, Y., 2017. Iodate in calcite and vaterite: insights from synchrotron X-ray absorption spectroscopy and first-principles calculations. Geochim. Cosmochim. Acta 198, 218–228.
Pohl, A., Lu, Z., Lu, W., Stockey, R.G., Elrick, M., Li, M., Desrochers, A., Shen, Y., He, R., Finnegan, S., Ridgwell, A., 2021. Vertical decoupling in Late Ordovician anoxia due to reorganization of ocean circulation. Nat. Geosci. 14, 868–873.
Poulton, S.W., Canfield, D.E., 2005. Development of a sequential extraction procedure for iron: implications for iron partitioning in continentally derived particulates. Chem. Geol. 214, 209–221.
Ren, H., Yang, R., Gao, J., Cheng, W., Wei, H., 2015. Enrichment regularities for iodine concentration in phosphorite of Doushantuo Formation of Late Ediacaran in Guizhou Province, SW China. Arab. J. Geosci. 8, 5423–5437.
Rue, E.L., Smith, G.J., Cutter, G.A., Bruland, K.W., 1997. The response of trace element redox couples to suboxic conditions in the water column. Deep Res. Part I Oceanogr. Res. Pap. 44, 113–134.
Sanders, C., Grotzinger, J., 2021. Sedimentological and stratigraphic constraints on depositional environment for Ediacaran carbonate rocks of the São Francisco Craton: implications for phosphogenesis and paleoecology. Precambrian Res. 363.
Schmitz, G., 2000. Kinetics of the dushman reaction at low I- concentrations. Phys. Chem. Chem. Phys. 2, 4041–4044.
Shang, M., Tang, D., Shi, X., Zhou, L., Zhou, X., Song, H., Jiang, G., 2019. A pulse of oxygen increase in the early Mesoproterozoic Ocean at ca. 1.57–1.56 Ga. Earth Planet. Sci. Lett. 527, 115797.
Sholkovitz, E.R., Landing, W.M., Lewis, B.L., 1994. Ocean particle chemistry: the fractionation of rare earth elements between suspended particles and seawater. Geochim. Cosmochim. Acta 58, 1567–1579.
Takaku, Y., Shimamura, T., Masuda, K., Igarashi, Y., 1995. Iodine determination in natural tap water using inductively coupled plasma mass spectrometry. Anal. Sci. 11, 823–827.
Tang, D., Fang, H., Shi, X., Liang, L., Zhou, L., Xie, B., Huang, K., Zhou, X., Wu, M., Riding, R., 2023. Mesoproterozoic molar tooth structure related to increased marine oxygenation. J. Geophys. Res. Biogeosci. 128, 1–18.
Tessier, A., Campbell, P.G.C., Bisson, M., 1979. Sequential extraction procedure for the speciation of particulate trace metals. Anal. Chem. 51, 844–851.
Tokunaga, K., Takahashi, Y., Tanaka, K., Kozai, N., 2021. Effective removal of iodate by coprecipitation with barite: behavior and mechanism. Chemosphere 266, 129104.
Tostevin, R., 2021. Cerium Anomalies and Paleoredox, Elements in Geochemical Tracers in Earth System Science. Cambridge University Press.
Tostevin, R., Shields, G.A., Tarbuck, G.M., He, T., Clarkson, M.O., Wood, R.A., 2016. Effective use of cerium anomalies as a redox proxy in carbonate-dominated marine settings. Chem. Geol. 438, 146–162.
Webb, G.E., Kamber, B.S., 2000. Rare earth elements in Holocene reefal microbialites: a new shallow seawater proxy. Geochim. Cosmochim. Acta 64, 1557–1565.
Wei, H., Wang, X., Shi, X., Jiang, G., Tang, D., Wang, L., An, Z., 2019. Iodine content of the carbonates from the Doushantuo Formation and shallow ocean redox change on the Ediacaran Yangtze Platform, South China. Precambrian Res. 322, 160–169.
Winkelbauer, H., Cordova-Rodriguez, K., Reyes-Macaya, D., Scott, J., Glock, N., Lu, Z., Hamilton, E., Chenery, S., Holdship, P., Dormon, C., Hoogakker, B., 2021. Foraminifera iodine to calcium ratios: approach and cleaning. Geochem. Geophys. Geosyst. 22, 1–11.
Wong, G.T.F., Brewer, P.G., 1977. The marine chemistry of iodine in anoxic basins. Geochim. Cosmochim. Acta 41, 151–159.
Wörndle, S., Crockford, P.W., Kunzmann, M., Bui, T.H., Halverson, G.P., 2019. Linking the Bitter Springs carbon isotope anomaly and early Neoproterozoic oxygenation through I/[Ca + Mg] ratios. Chem. Geol. 524, 119–135.
Wotte, T., Shields-Zhou, G.A., Strauss, H., 2012. Carbonate-associated sulfate: experimental comparisons of common extraction methods and recommendations toward a standard analytical protocol. Chem. Geol. 326–327, 132–144.
Xie, Y., McDonald, M.R., Margerum, D.W., 1999. Mechanism of the reaction between iodate and iodide ions in acid solutions (dushman reaction). Inorg. Chem. 38, 3938–3940.
Zhang, K., Shields, G.A., 2022. Sedimentary Ce anomalies: secular change and implications for paleoenvironmental evolution. Earth-Sci. Rev. 229, 104015.
Zhang, K., Shields, G.A., 2023. Early diagenetic mobilization of rare earth elements and implications for the Ce anomaly as a redox proxy. Chem. Geol. 635, 121619.
Zhang, K., Zhu, X., Yan, B., 2015. A refined dissolution method for rare earth element studies of bulk carbonate rocks. Chem. Geol. 412, 82–91.
Zhang, F., Lenton, T.M., del Rey, Á., Romaniello, S.J., Chen, X., Planavsky, N.J., Clarkson, M.O., Dahl, T.W., Lau, K.V., Wang, W., Li, Z., Zhao, M., Isson, T., Algeo, T. J., Anbar, A.D., 2020. Uranium isotopes in marine carbonates as a global ocean paleoredox proxy: a critical review. Geochim. Cosmochim. Acta 287, 27–49.
Zhou, X., Thomas, E., Rickaby, R.E.M., Winguth, A.M.E., Lu, Z., 2014. I/Ca evidence for upper ocean deoxygenation during the PETM. Paleoceanography 29, 964–975.